CrossMark

ORIGINAL ARTICLE

Dimensions of the cervical neural foramen in conditions of spinal deformity: an ex vivo biomechanical investigation using specimen-specific CT imaging

Zachary A. Smith[1] · Saeed Khayatzadeh[2] · Joshua Bakhsheshian[3] ·
Michael Harvey[1] · Robert M. Havey[2,4] · Leonard I. Voronov[2,4] · Muturi G. Muriuki[2] ·
Avinash G. Patwardhan[2,4]

Abstract

Purpose Patients with cervical spondylosis commonly present with neck pain, radiculopathy or myelopathy. As degenerative changes progress, multiple factors including disc height loss, thoracic kyphosis, and facetogenic changes can increase the risk of neural structure compression. This study investigated the impact of cervical deformity including forward head posture (FHP) and upper thoracic kyphosis, on the anatomy of the cervical neural foramen.

Methods Postural changes of 13 human cervical spine specimens (Occiput-T1, age 50.6 years; range 21–67) were assessed in response to prescribed cervical sagittal malalignments using a previously reported experimental model. Two characteristics of cervical sagittal deformities, C2–C7 sagittal vertical alignment (SVA) and sagittal angle of the T1 vertebra (T1 tilt), were varied to create various cervical malalignments. The postural changes were documented by measuring vertebral positions and orientations. The vertebral motion data were combined with specimen-specific CT-based anatomical models, which allowed assessments of foraminal areas of subaxial cervical segments as a function of increasing C2–C7 SVA and changing T1 tilt.

Results Increasing C2–C7 SVA from neutral posture resulted in increased neural foraminal area in the lower cervical spine (largest increase at C4–C5: 13.8 ± 15.7 %, $P < 0.01$). Increasing SVA from a hyperkyphotic posture (greater T1 tilt) also increased the neural foraminal area in the lower cervical segments (C5–C6 demonstrated the largest increase: 13.4 ± 9.6 %, $P < 0.01$). The area of the cervical neural foramen decreased with increasing T1 tilt, with greater reduction occurring in the lower cervical spine, specifically at C5–C6 (-8.6 ± 7.0 %, $P < 0.01$) and C6–C7 (-9.6 ± 5.6 %, $P < 0.01$).

Conclusion An increase in thoracic kyphosis (T1 tilt) decreased cervical neural foraminal areas. In contrast, an increase in cervical SVA increased the lower cervical neural foraminal areas. Patients with increased upper thoracic kyphosis may respond with increased cervical SVA as a compensatory mechanism to increase their lower cervical neural foraminal area.

Keywords Cervical spine deformity · Radiculopathy · Forward head posture · Neck pain · Sagittal vertical alignment

✉ Avinash G. Patwardhan
apatwar@lumc.edu

[1] Department of Neurological Surgery, Northwestern Feinberg School of Medicine, Chicago, IL, USA

[2] Musculoskeletal Biomechanics Laboratory, Edward Hines, Jr. VA Hospital, Hines, IL 60141, USA

[3] Department of Neurological Surgery, Keck School of Medicine, University of Southern California, Los Angeles, CA, USA

[4] Department of Orthopaedic Surgery and Rehabilitation, Loyola University Medical Center, 2160 S. First Avenue, Maywood, IL 60153, USA

Abbreviations
CT   Computed tomography
FHP   Forward head posture
SVA   Sagittal vertical alignment
3D   Three-dimensional
MR   Magnetic resonance

Introduction

Cervical spine degenerative disease is a common problem in our aging population, which can lead to substantial pain and functional disability [1]. As degeneration progresses over time, there are multiple factors that distort the normal anatomy of the cervical spine. As a patient's discs lose height, the facets hypertrophy, and bony spurring may occur. It has been previously shown that these common degenerative changes may negatively impact the size of the cervical neural foramen [2]. However, the impact of cervical deformity on the size of the neural foramen has not been thoroughly studied.

Abnormal neck alignment, or cervical deformity, can be quantified by multiple radiographic techniques. One common measure is the sagittal vertical alignment (SVA) of C2 vertebra relative to C7 (C2–C7 SVA). The SVA is calculated as the horizontal distance from a C2 plumb line to the C7 vertebral body (Fig. 1) [3, 4]. A second measure is the T1 sagittal angle (T1 tilt) [5]. This calculates the angle between a horizontal line and the superior endplate of T1. The T1 tilt is a surrogate for the degree of thoracic kyphosis. Previously, our laboratory reported an ex vivo biomechanical cervical model that can be used to evaluate the biomechanical consequences of cervical neck deformity by modifying these two key variables [6]. The cervical model serves as a platform to evaluate how these components of deformity impact the biomechanics of the cervical spine. We used reconstructed three-dimensional (3D) computed tomography (CT) modeling, to evaluate the impact of deformity on the nerve root foramen.

The dimensions of the cervical neural foramen have never been previously quantified in relation to the SVA or T1 tilt. In this study, we report neural foraminal areas of the cervical segments with varying C2–C7 SVA and T1 tilt, obtained through dynamic specimen-specific CT examinations of cadaveric specimens.

Methods

Specimen preparation

The experiments were performed using 13 fresh-frozen cadaveric cervical spine specimens (occiput-T1) of adult donors (median age 56 years; range 21–67; 9 males, 4 females) (Table 1) from an age range with a high incidence of cervical radiculopathy symptoms [7]. Specimens were thawed and stripped of the paraspinal musculature while preserving the discs, facet joints, and osteoligamentous structures. Each disc was scored with a five-point disc degeneration scale based on MRI findings [8]. Grades 1–3 were considered normal to low level of degeneration, while grades 4–5 were considered moderate to severe level of degeneration.

Specimen-specific anatomic model

Radiopaque spheres (fiduciary markers) were rigidly attached to each vertebral body prior to CT imaging. After obtaining an axial fine-slice (0.63 mm) CT scan (Light-Speed VPT, GE Medical Systems), three-dimensional (3D)
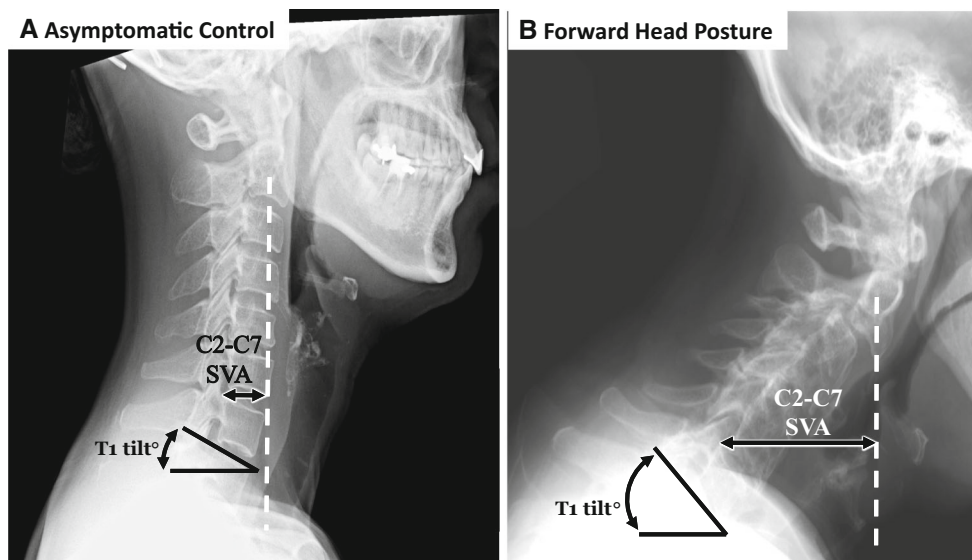

Fig. 1 Cervical sagittal alignment measurements in an asymptomatic patient (a) and a patient with forward head posture (b). C2–C7 SVA is defined as the distance from the posterior superior corner of C7 to a plumb line drawn from the center of the C2 vertebral body. T1 tilt is defined as the angle between a *horizontal line* and the superior end plate of T1

Table 1 Specimen demographics

Specimen	Age (years)	Sex	Height (inches)	Weight (lbs)	Cause of death
1	59	F	67	181	Cardiac arrest
2	56	M	73	125	Lung cancer
3	56	M	74	325	Sepsis
4	57	F	65	110	Breast cancer
5	67	F	64	220	Colon cancer
6	63	M	66	135	Multiorgan failure
7	40	M	NA	NA	NA
8	21	M	70	120	CHF
9	21	M	70	140	Drug overdose
10	50	M	72	205	CAD
11	59	M	NA	NA	NA
12	57	F	NA	NA	NA
13	52	M	NA	NA	Respiratory distress syndrome
Mean (SD)	50.6 (14.6)	9 M/4 F	69 (3.7)	173.4 (68.9)	
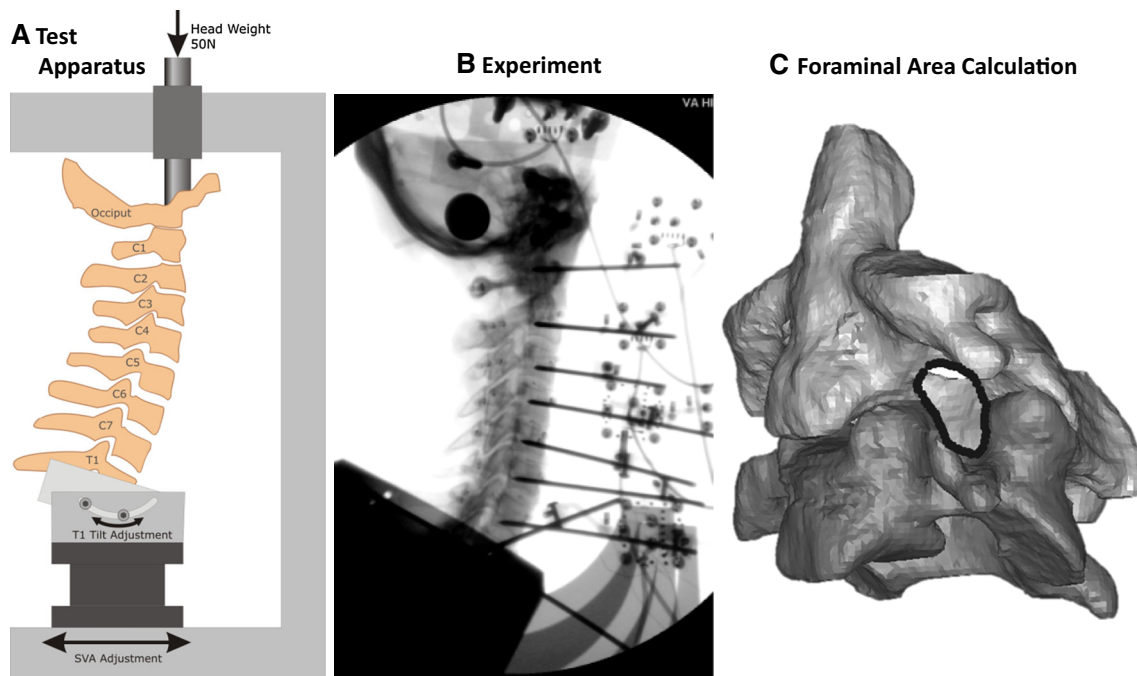
Fig. 2 Dynamic 3D specimen specific anatomical model. The dynamic model includes the following steps: **a** test design, **b** experiment and **c** neural foraminal area calculation

specimen-specific anatomical model of each vertebral body were reconstructed using the Mimics software package (Materialise, Inc., Plymouth, MI) (Fig. 2).

Test apparatus

Specimens were mounted in an apparatus that allowed independent adjustment in the sagittal plane of the horizontal offset distance between the head center of mass and

T1 (C0-T1 SVA) and T1 tilt (Fig. 2a). Previous literature has defined SVA as "Sagittal vertebral axis". In this manuscript we redefined the term SVA as sagittal vertical alignment, which is a measure of the vertical alignment between vertebrae with units of millimeters (mm).

The T1 vertebra was anchored in cement and was attached to the tilting and translating base of the test apparatus. A 5 kg mass was attached to the occiput to mimic the weight of an average head [9]. The sagittal tilt of

the occiput was fixed to remain consistent with horizontal gaze regardless of sagittal imbalance [10].

Given that the specimens contained the occiput and not the entire skull, the determination of horizontal gaze was made based on the orientation of the foramen magnum. Been et al. previously demonstrated that the foramen magnum is oriented to the horizontal plane by $10.2° \pm 6.7°$ (facing caudally and slightly anteriorly) [11]. Other studies have reported values ranging from $3.4° \pm 6.5°$ to $8.2° \pm 6.5°$ [4, 12]. In the present study we used fiduciary markers attached to the occiput to determine the inclination of the foramen magnum. The foramen magnum was then defined in relation to the fiduciary markers in the reconstructed CT model. During experimentation, the radiopaque marker locations were used to orient the occiput relative to the horizontal plane.

3D optoelectronic motion measurement targets (Optotrak, Certus, Northern Digital Inc., Waterloo, ON, Canada) were rigidly attached to each vertebral body to record their motion during the experiments (Fig. 3). Specimens were initially placed in a neutral posture (C0-T1 SVA = 20 mm, T1 angle = 23°), which was based on normative data from asymptomatic subjects [5, 12, 13]. Specimen-specific adjustments to the values of the C0-T1 SVA, T1 tilt, and sagittal tilt of the foramen magnum were necessary to keep the moment values in the specimen's neutral posture below a threshold of ± 0.2 Nm.
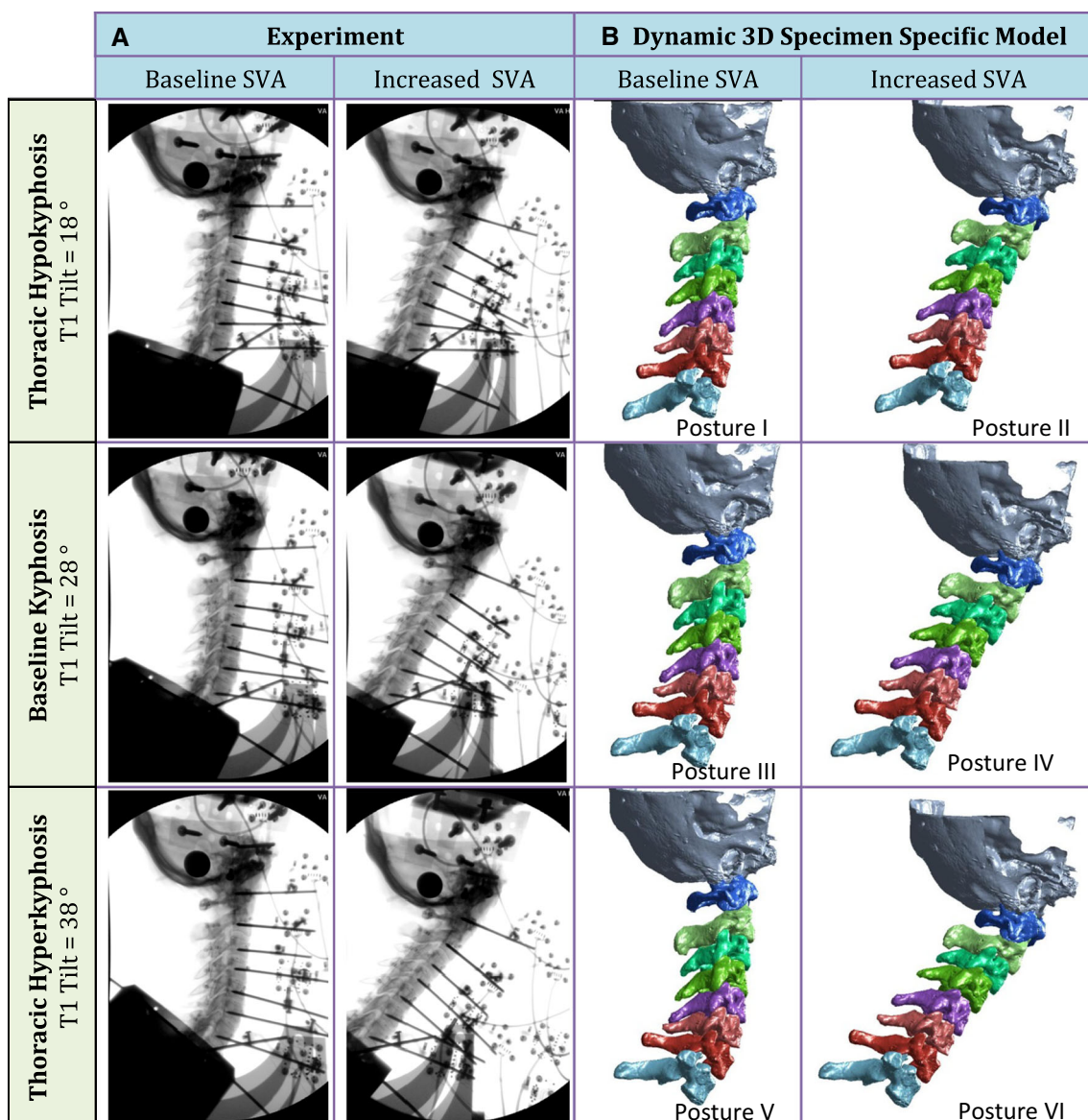
Fig. 3 A spine specimen in various postures created by varying the SVA and T1 tilt. **a** Digital fluoroscopy images of the specimen in the different combinations of malalignment postures. **b** Specimen specific CT anatomical model of the same specimen and postures

Table 2 Standard test protocol for each specimen

	T1 tilt		C2-C7 SVA	
1	Baseline T1 tilt −10°	(fixed)	Baseline SVA → Baseline SVA +40 mm	(varied)
	[Thoracic hypokyphosis]		[Baseline FHP → Severe FHP]	
2	Baseline T1 tilt	(fixed)	Baseline SVA → Baseline SVA +40 mm	(varied)
	[Baseline thoracic kyphosis]		[Baseline FHP → Severe FHP]	
3	Baseline T1 tilt +10°	(fixed)	Baseline SVA → Baseline SVA +40 mm	(varied)
	[Thoracic hyperkyphosis]		[Baseline FHP → Severe FHP]	
4	Baseline T1 tilt −10° → Baseline T1 tilt +10°	(varied)	Baseline SVA	(fixed)
	[Thoracic hypokyphosis → thoracic hyperkyphosis]		[Baseline FHP]	
5	Baseline T1 tilt −10° → Baseline T1 tilt +10°	(varied)	Baseline SVA + 23 mm	(fixed)
	[Thoracic hypokyphosis → thoracic hyperkyphosis]		[Severe FHP]	

Each specimen has different baseline values: mean baseline (C2–C7) SVA = 21.7 ± 7.5 mm, mean baseline T1 angle = 25.3° ± 7.2°

The amount of flexion moment at the base was not allowed to exceed 3.0 Nm

Test parameters and protocol

Tests were performed with various malalignment combinations (Table 2). Sagittal malalignment was achieved by varying the following independent variables: C2–C7 SVA (the horizontal offset distance between the C2 plumb line and C7 vertebral body) and T1 tilt (in the sagittal plane the angle that the T1 superior endplate makes with the horizon). One variable was kept constant while varying the other (Table 2) [6]. The T1 tilt was set to three values: hypokyphosis, baseline (specimen's neutral posture) and hyperkyphosis. The C2–C7 SVA, which is also a measure of forward head posture (FHP), was set to two values: baseline and severe FHP.

Starting with the baseline posture of the specimen, the magnitude of C0-T1 SVA was increased and changes in angular and translational alignments of C1–C7 vertebrae were measured using optoelectronic sensors. While the head was constrained to horizontal gaze, the cervical segments accommodated the increasing anterior head offset. The test was stopped when the moment measured by the load-cell placed beneath T1 reached a limit of 3 Nm. This stopping criterion was used to minimize the risk of soft tissue damage that may occur due to repeated testing [14, 15]. The effect of T1-tilt on postural realignment was then assessed by changing the T1-tilt angle until the test stopping criterion was met. The response of the spine to combinations of the two independent variables was studied (Table 2).

Specimen-specific kinematic model

In this step, the specimen-specific 3D CT-based anatomic model was animated using the vertebral motion data recorded by the optoelectronic targets. To combine the motion data and 3D anatomic model, the fiduciary markers were registered in relation to the optoelectronic target, which were attached to their respective vertebral bodies. This registration provided the ability to track the fiduciary markers throughout the specimens' range of motion. This process resulted in a computer generated 3D representation of the specimen's CT reconstruction moving through its range of motion in response to the changing SVA and T1 tilt (Fig. 3). Details of this methodology can be found in a prior published study, Havey et al. [16].

Foraminal area measurement

The left and right foraminal boundaries of each motion segment were defined by identifying points on the 3D anatomic model, which included: the pedicle and pars interarticularis superiorly, the facet joint posteriorly, the pedicle and posterior wall of the vertebra below inferiorly, the intervertebral disc and posterior wall of vertebra above anteriorly (Fig. 2c). The tracings of the neural foramen were done manually for the neutral posture. The oblique angle that provided the largest view of the neural foramen area was utilized for defining the neural foramen boundaries. The tracing was projected onto a plane which was orthogonal to the above referenced oblique direction. As the vertebrae moved in response to a prescribed sagittal malalignment, the relationship between the bony landmarks that defined the cranial and caudal neural foramen boundaries changed, affecting the neural foraminal area, which was calculated using the specimen-specific kinematic model. Two investigators independently agreed upon the tracings of each neural foramen boundary and viewing angle that corresponded to the maximum neural foraminal area.
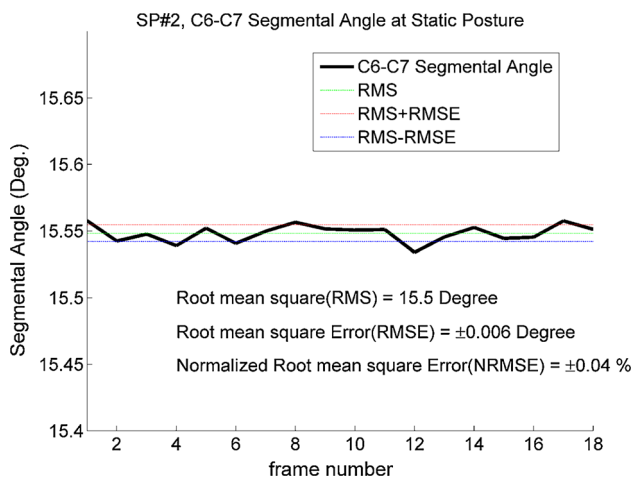
Fig. 4 Root mean square (RMS) error of segmental angle in static posture
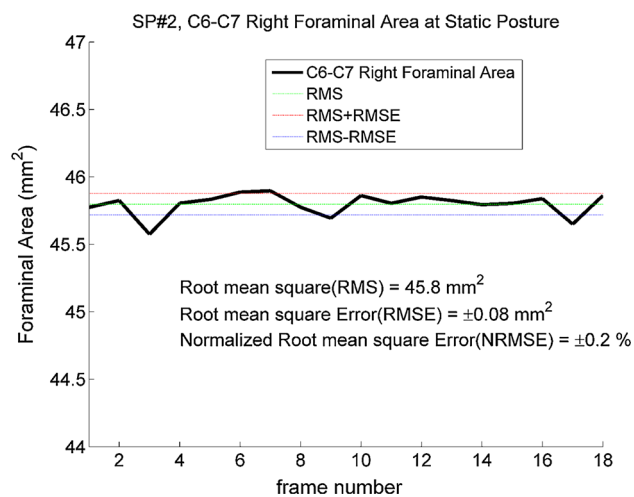
Fig. 5 RMS error of neural foraminal area in static posture

Error estimation

Root mean square accuracy of measuring 3D motion of anatomical features was determined to be ±0.44 mm. Error in translation due to the dynamic tracking of points was 0.14 mm, while the error due to probe registration of anatomical points was 0.40 mm. This was primarily limited by the CT scan voxel size of $(0.29 \times 0.29 \times 0.625$ mm). While the specimen was kept stationary, the RMSE (root mean square error) of the recorded segmental angle of a sample segment, C6–C7, was ±0.006° and, the RMSE of the calculated neural foraminal area of the same segment was ±0.08 mm^2 (Figs. 4, 5). The RMSE of the neural foraminal area as the specimen posture changed in response to increasing SVA was ±0.1 mm^2 (Fig. 6).
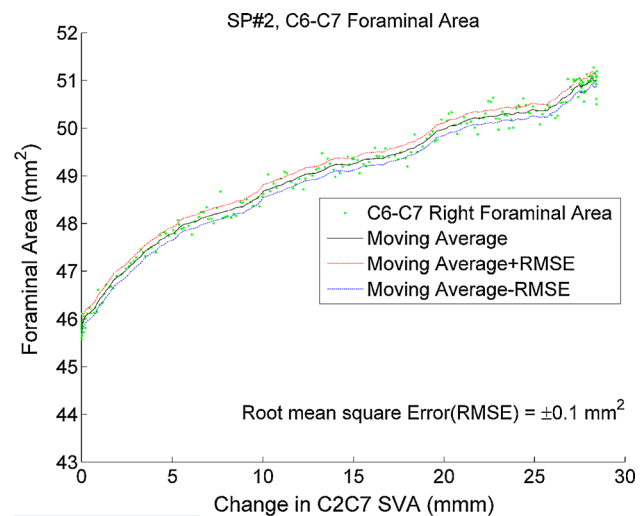
Fig. 6 RMS error of neural foraminal area throughout the increasing SVA experiment on a representative specimen

Statistical data analysis

All data were analyzed to obtain descriptive statistics and a repeated-measures analysis of variance was performed to compare the foraminal sizes for different values of independent variables. The neural foraminal areas were processed to obtain the percent change in area relative to the neutral posture, unless otherwise stated.

The native sagittal alignment and tissue stiffness of each specimen influenced the maximum SVA that could be achieved before the stopping criterion of 3 Nm was reached. For example, the maximum attainable SVA (before reaching the stopping criteria) ranged from 31 to 68 mm for a neutral T1 tilt value. The native segmental alignment also influenced the neural foraminal areas in the neutral posture of the specimen and the magnitude of changes in neural foraminal areas caused by changing SVA and T1 tilt. The variability in native alignment and tissue stiffness are reflected in the variability of the results presented in the study. All samples were able to demonstrate an increase of 16 mm in C2–C7 SVA, and therefore this point was utilized for further statistical analysis.

Results

Biomechanical model characteristics

As explained in "Methods", degenerative changes in the discs were graded based on MRI scans. In our samples, the grade ranged between 2 and 3, indicating mild degenerative changes in the discs.

In neutral posture, the average neural foraminal area ranged from 33.0 to 55.5 mm^2 and the mean neural foraminal
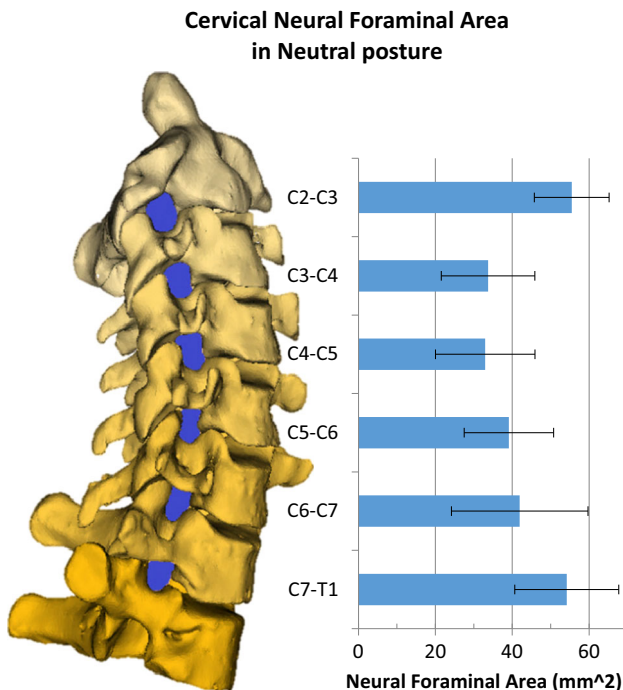
Fig. 7 Mean neural foraminal areas of cervical segments in the neutral posture of all specimens (*n* = 13). Neutral posture is depicted as posture III in Fig. 3
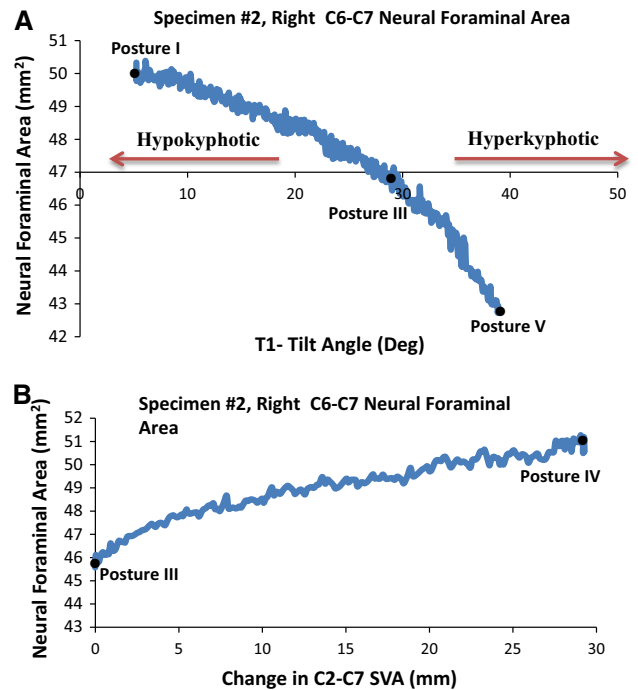
Table 3 Mean cervical neural foraminal areas measured in the neutral posture (*n* = 13)

Level	C2–C3	C3–C4	C4–C5	C5–C6	C6–C7	C7–T1
Mean (mm^2)	55.5	33.7	33.0	39.1	42.0	54.2
SD	9.7	12.2	12.9	11.6	17.7	13.5

area of all cervical segments was 43.2 mm^2 (±15.6 mm^2). The mean neural foraminal area for each level was C2–C3: 54.2 mm^2 (±13.5 mm^2) C3–C4: 41.9 mm^2 (±17.7 mm^2), C4–C5: 39.1 mm^2 (±11.6 mm^2), C5–C6: 33.0 mm^2 (±12.9 mm^2), C6–C7: 33.7 mm^2 (±12.2 mm^2) and C7-T1: 55.5 mm^2 (±9.7 mm^2) (Fig. 7; Table 3).

Area of the cervical neural foramen decreases with increasing T1 tilt

There was an inverse relationship between the neural foraminal areas and T1 tilt angle changes. As the T1 tilt increased from the neutral position, a decrease in the neural foraminal area was observed in all samples at all segments (Fig. 8a). During hyperkyphosis, peak neural foraminal area narrowing occurred at the lower cervical spine, specifically at C5–C6 ($P < 0.01$) and C6–C7 ($P < 0.01$) (Table 4; Fig. 9a). In contrast, there was minimal change in the upper cervical segments.

Fig. 8 Representative neural foraminal area vs. **a** T1 tilt and **b** changes in C2–C7 SVA on a specific cervical neural foramen. Please see Fig. 3 and Table 2 for illustrative depiction of the various postures tested

When the T1 tilt was decreased from the neutral position, a progressive increase in the neural foraminal area was observed in all samples at all segments. At T1 tilt of 13° the C5–C6 segment demonstrated the largest increase from neutral position ($P < 0.01$) (Table 4).

Area of the subaxial cervical neural foramen increases with increasing C2–C7 SVA

Increasing the C2–C7 SVA from the neutral position had different effects on lower and upper cervical neural foraminal areas (Table 4). Increases in the neural foraminal areas of mid-to-lower cervical segments were observed. Representative changes in C6–C7 foramen in relation to change in C2–C7 SVA are shown in Fig. 8b for an SVA change of up to 30 mm. In contrast, a minimal change was observed in the upper cervical segments.

All specimens were able to withstand an increase of 16 mm in C2–C7 SVA, therefore this point was utilized for statistical comparative analysis. The C4–C5 segment demonstrated the largest increase in neural foraminal area for an increase in C2–C7 SVA of 16 mm from neutral position ($P < 0.01$) (Fig. 9b). We also evaluated neural foraminal areas for specimen-specific maximum SVA values corresponding to the maximum flexion moment (3 Nm) for all specimens, instead of using a fixed value of SVA increase (16 mm) for each specimen. The comparison

Table 4 Summary of percentage changes in foraminal area from a posture to another posture

	Initial posture Final posture	Neutral (posture III) Hyperkyphosis (posture V) (%)	Neutral (posture III) Hypokyphosis (posture I) (%)	Neutral (posture III) Forward head posture (posture IV) (%)	Hyperkyphosis (posture V) Hyperkyphosis and forward head posture (posture VI) (%)
Level	C2–C3	0.1 ± 0.5	0.9 ± 1.8	−0.3 ± 1.0	−0.4 ± 1.0
	C3–C4	−0.4 ± 1.0	**4.5 ± 2.4**	0.1 ± 2.3	−0.9 ± 3.7
	C4–C5	**−2.7 ± 2.2**	**9.2 ± 3.3**	**13.8 ± 15.7**	**3.4 ± 3.6**
	C5–C6	**−8.6 ± 7.0**	**9.4 ± 8.7**	**9.6 ± 4.2**	**13.4 ± 9.6**
	C6–C7	**−9.6 ± 5.6**	2.0 ± 4.1	**5.2 ± 4.0**	**11.4 ± 7.9**
	C7-T1	−1.6 ± 3.2	0.0 ± 0.7	*2.0 ± 2.8*	*4.3 ± 4.8*

Bold values: P value <0.01, italic values: P value <0.05. Figure 3 depicts the different posture numbers

Fig. 9 Relative percent changes in neural foraminal area with varying **a** T1 tilt only, **b** cervical SVA only or **c** T1 tilt and cervical SVA. See Fig. 3 and Table 2 for illustrative depiction of the various postures tested
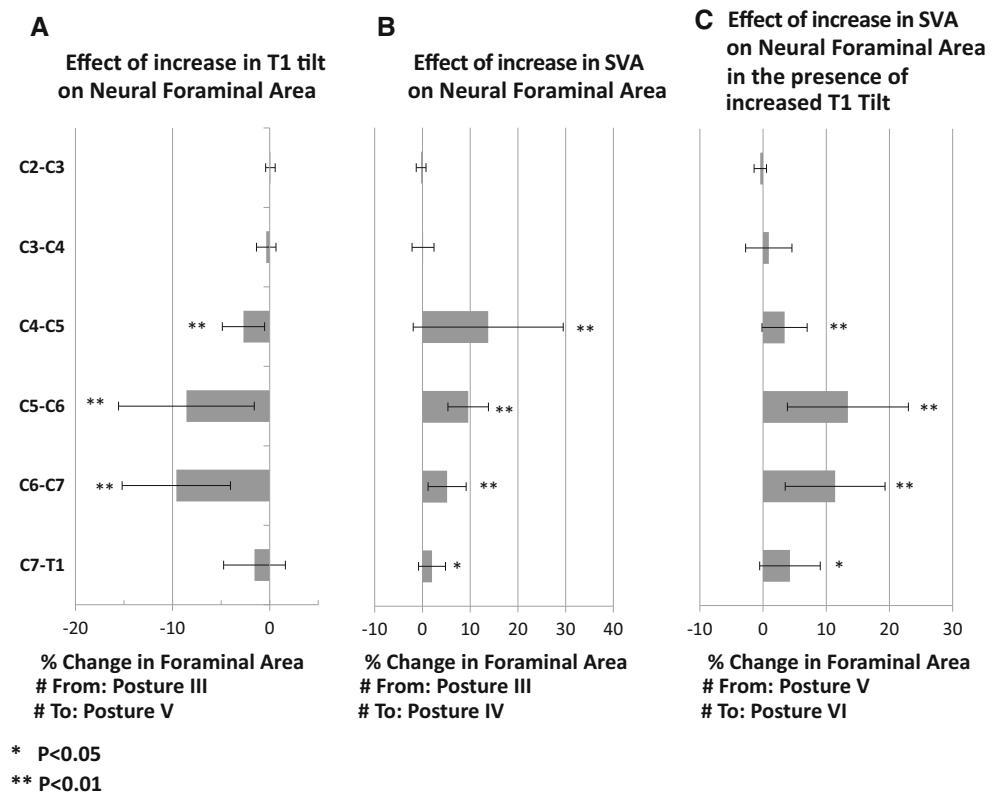
showed that both criteria yield similar patterns of changes in neural foraminal area at all segments (Fig. 10).

Increasing SVA from a thoracic hyperkyphotic T1 posture also increased the neural foraminal area in the mid-to-lower cervical segments (Fig. 9c; Table 4). In this case, the C5–C6 segment demonstrated the greatest increase in neural foraminal area from the neutral posture ($P < 0.01$).

Discussion

Cervical degenerative disc disease can often lead to the development of cervical deformity. These patients will frequently have co-existing symptoms of nerve root compression. While radiographic measurements of cervical deformity, C2-C7 SVA and T1 tilt, have been shown in recent retrospective studies to correlate with clinical outcome scores [3, 5, 17], the impact of these variables on the anatomy of the neural foramen remains unknown. It is important to understand how the neural foramen change in deformity as this will help us identify anatomical drivers of a patient's symptoms, informing both our understanding of prognosis and treatment [18–20]. In this study, we found that thoracic kyphosis had a negative impact on the size of the neural foramen. As thoracic kyphosis (T1 tilt) increased, the neural foramen decreased in size. Conversely, as the C2–C7 SVA increased (a more forward head posture), the neural foramen size increased. These changes
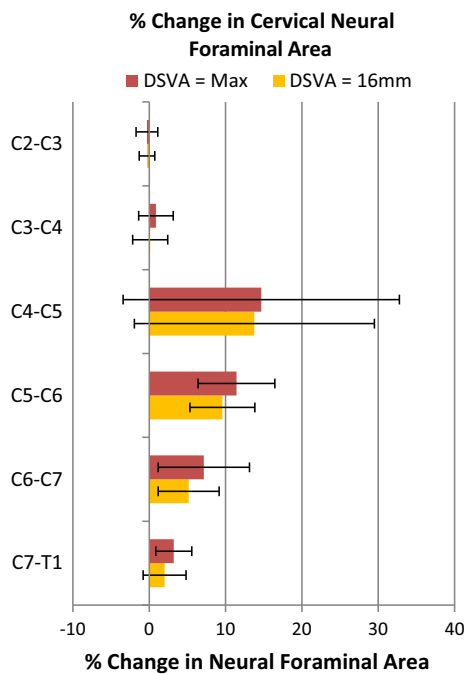
Fig. 10 Percent change in neural foraminal area assessed for a fixed ΔSVA value of 16 mm for all specimens vs. for specimen-specific max SVA change

were most prominent in the lower cervical spine, a common site of clinical symptoms.

While symptoms of deformity can exist in isolation, patients with severe degenerative changes often will have symptomatic nerve root compression. It is important to note that imaging findings do not always correlate with radicular symptoms [21] and the potential impact of cervical sagittal alignment on the neural foraminal spaces is not well understood. In our study, when the specimen was placed in a posture of significantly increased thoracic kyphosis, the neural foraminal area of the lower cervical spinal segments decreased in size. When the specimen underwent an increase in SVA, the neural foraminal area increased in size. This change may be indicative of a compensatory mechanism, wherein a patient's forward head posture is a compensatory mechanism to relieve radicular symptoms (opens a constricted neural foramen). In the current study, variations in T1 tilt and cervical SVA led to larger changes in the neural foramen of the lower cervical region (C5–C7). In theory, this places the lower cervical roots at higher risk for compression [7].

In our biomechanical model, the greatest average change in the neural foraminal area in relation to high thoracic kyphosis was observed at C4–C5. This is an interesting finding given the presence of C5 palsy after some spinal operations [20]. The pathophysiology of C5 palsy is multifactorial and poorly understood, with the most common theory being posterior migration of the spinal

cord causing traction on the C5 nerve root [22]. The C5 nerve root is the shortest cervical nerve root, further contributing to its risk for injury. Importantly, the C4–C5 neural foramen are also smaller than most of the other subaxial cervical neural foramen in neutral posture (Fig. 7). Panjabi et al. also demonstrated in an ex vivo cadaveric model with lateral radiographs that peak neural foraminal area narrowing occurs at C4–C5 in extension postures [23]. Thus, the combination of a small neural foramen as well as its reduction in size with regional deformity, may place the C5 nerve root at highest anatomical risk.

Previous techniques used to evaluate cervical neural foraminal dimensions included direct measurement with blunt probes [24], foramen occlusion transducers [25], and measurements with CT or MR imaging in static postures [26–28]. Yoo et al. investigated the neural foraminal areas of C5–C7 in cadaveric specimens with blunt probes. Their findings showed that neural foraminal areas significantly increased during flexion and decreased during extension [24]. Nuckley et al. investigated the foramen integrity by recordings from transducers in the neural foraminal space. The integrity of the neural foramen space was compromised with extension [25]. Humphreys et al. investigated changes in the foraminal space at C5–C6 in cadaver specimens during flexion and traction with CT imaging. The authors demonstrated a significant increase in neural foraminal area during flexion [26–28].

The neural foraminal area changes during flexion and extension were also confirmed in healthy subjects with MR imaging [28] and CT imaging [27, 29]. Muhle et al. assessed flexion–extension in the cervical spine of 30 healthy persons using kinematic MR imaging [28] and demonstrated a significant difference between flexion and extension, where flexion caused a widening of the foraminal space (+30 %) and extension caused narrowing (−19 %). Specifically, Muhle et al. noted C4–C5 neural foraminal area increased by 18 % and by 30 % in lower cervical segments with maximum flexion. With maximum extension, the neural foraminal area of C4-T1 similarly decreased by ∼19 %. Kitagawa et al. acquired CT images of seven healthy volunteers at neutral position, maximum extension, and maximum flexion. The authors reconstructed the images in the oblique plane perpendicular to the long axis of each neural foramen from C3 to C7 but did not discuss the segments independently. Flexion significantly increased the neural foraminal area (+28 %) and extension significantly decreased the neural foraminal area (17–22 %). Overall, Kitagawa et al. and Muhle et al. observed similar values of neural foraminal areas when compared to our ex vivo model (Fig. 11). Results from Panjabi's ex vivo study also corroborated these values [23]. Together, these findings demonstrate that the morphologic

Cervical Neural Foraminal Area in Neutral posture
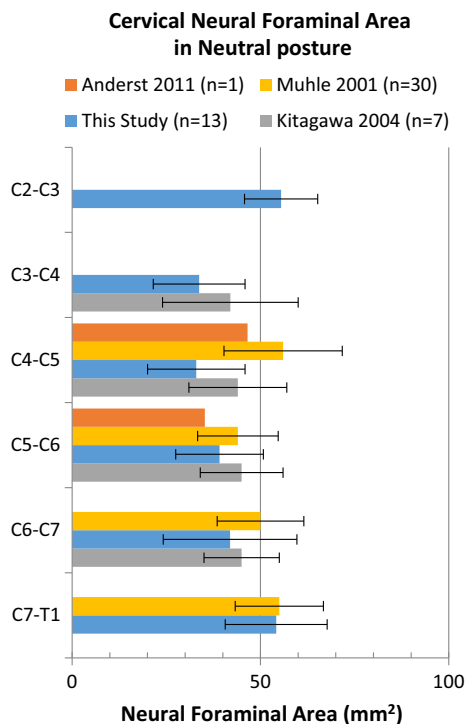
Fig. 11 Comparison of changes in the cervical neural foraminal area of this study and previously published in-vivo studies

changes in the cervical neural foramen in vivo are comparable to ex vivo cadaveric studies.

The main scientific contribution of our study is that we investigated the effects of cervical spinal imbalance (increasing C2-C7 SVA and T1 tilt) on cervical neural foraminal areas of cervical segments from C2 to C3 to C7-T1. Previous studies have assessed neural foraminal space primarily during flexion–extension motions of the neck. The results of the present study describing the effects of cervical sagittal malalignment on neural foraminal space provide data that has not been previously reported in the literature.

This study is not without limitations. We acknowledge the study is limited by its ex vivo nature. However, the utilization of an ex vivo model provided a controlled environment which is highly reproducible. Variables of deformity cannot be modified with precision in the clinical setting. The lack of paraspinal musculature may also be considered a limitation. However, comparing our ex vivo data to findings of in vivo studies suggest that the neck musculature may not play a predominant role in the pattern of neural foraminal changes. Lastly, our specimen specific CT model focuses solely on the bony anatomy of the neural foramen. It is well established that soft-tissue structures, namely the disc and ligaments, play a critical role in nerve root compression. Further studies are needed to incorporate the role of these soft-tissue structures.

Conclusions

In an ex vivo biomechanical model with specimen-specific CT images, the size of the subaxial neural foramen can be calculated in simulated positions of cervical deformity. With increasing upper thoracic kyphosis, the dimensions of the cervical neural foramen decrease in size. This is most pronounced in the lower cervical spine. In contrast, an increase in cervical SVA increases the area of the neural foramen. These findings may imply that a forward head posture is a compensatory mechanism to provide sufficient space for the neural structures as thoracic kyphosis progresses.

References

1. Ferrara LA (2012) The biomechanics of cervical spondylosis. Adv Orthop 2012:493605. doi:10.1155/2012/493605
2. Humphreys SC, Hodges SD, Patwardhan A, Eck JC, Covington LA, Sartori M (1998) The natural history of the cervical foramen in symptomatic and asymptomatic individuals aged 20–60 years as measured by magnetic resonance imaging. A descriptive approach. Spine 23:2180–2184
3. Tang JA, Scheer JK, Smith JS, Deviren V, Bess S, Hart RA, Lafage V, Shaffrey CI, Schwab F, Ames CP, ISSG (2012) The impact of standing regional cervical sagittal alignment on outcomes in posterior cervical fusion surgery. Neurosurgery 71:662–669. doi:10.1227/NEU.0b013e31826100c9 **(discussion 669)**
4. Hardacker JW, Shuford RF, Capicotto PN, Pryor PW (1997) Radiographic standing cervical segmental alignment in adult volunteers without neck symptoms. Spine 22:1472–1480 **(discussion 1480)**
5. Knott PT, Mardjetko SM, Techy F (2010) The use of the T1 sagittal angle in predicting overall sagittal balance of the spine. Spine J Off J N Am Spine Soc 10:994–998. doi:10.1016/j.spinee.2010.08.031
6. Patwardhan AG, Havey RM, Khayatzadeh S, Muriuki MG, Voronov LI, Carandang G, Nguyen NL, Ghanayem AJ, Schuit D, Patel AA, Smith ZA, Sears W (2015) Postural consequences of cervical sagittal imbalance—a novel laboratory model. Spine. doi:10.1097/BRS.0000000000000877
7. Radhakrishnan K, Litchy WJ, O'Fallon WM, Kurland LT (1994) Epidemiology of cervical radiculopathy. A population-based

study from Rochester, Minnesota, 1976 through 1990. Brain J Neurol 117(Pt 2):325–335

8. Miyazaki M, Hong SW, Yoon SH, Zou J, Tow B, Alanay A, Abitbol JJ, Wang JC (2008) Kinematic analysis of the relationship between the grade of disc degeneration and motion unit of the cervical spine. Spine 33:187–193. doi:10.1097/BRS.0b013e3181604501

9. Yoganandan N, Pintar FA, Zhang J, Baisden JL (2009) Physical properties of the human head: mass, center of gravity and moment of inertia. J Biomech 42:1177–1192. doi:10.1016/j.jbiomech.2009.03.029

10. Madsen DP, Sampson WJ, Townsend GC (2008) Craniofacial reference plane variation and natural head position. Eur J Orthod 30:532–540. doi:10.1093/ejo/cjn031

11. Been E, Shefi S, Zilka LR, Soudack M (2014) Foramen magnum orientation and its association with cervical lordosis: a model for reconstructing cervical curvature in archeological and extinct Hominin specimens. Adv Anthropol 2014

12. Nojiri K, Matsumoto M, Chiba K, Maruiwa H, Nakamura M, Nishizawa T, Toyama Y (2003) Relationship between alignment of upper and lower cervical spine in asymptomatic individuals. J Neurosurg 99:80–83

13. Gore DR, Sepic SB, Gardner GM (1986) Roentgenographic findings of the cervical spine in asymptomatic people. Spine 11:521–524

14. Martin S, Ghanayem A, Tzermiadianos M et al (2011) Kinematics of cervical total disc replacement adjacent to a two-level, straight vs. lordotic fusion. Spine (Phila Pa 1976) 36(17):1359–1366

15. Lee M, Dumonski M, Phillips F et al (2011) Disc replacement adjacent to cervical fusion: a biomechanical comparison of hybrid construct vs. two-level fusion. Spine (Phila Pa 1976) 36(23):1932–1939

16. Havey RM, Goodsitt J, Khayatzadeh S, Muriuki M, Potluri T, Voronov LI, Lomasney LM, Patwardhan AG (2015) Three-dimensional computed tomography based specimen-specific kinematic model for ex vivo assessment of lumbar neuroforaminal space. Spine (Phila Pa 1976) 40(14):E814–E822. doi: 10.1097/BRS.0000000000000959

17. Park JH, Cho CB, Song JH, Kim SW, Ha Y, Oh JK (2013) T1 slope and cervical sagittal alignment on cervical CT radiographs of asymptomatic persons. J Korean Neurosurg Soc 53:356–359. doi:10.3340/jkns.2013.53.6.356

18. Jenis LG, Banco S, Jacquemin JJ, Lin KH (2004) The effect of posterior cervical distraction on foraminal dimensions utilizing a screw-rod system. Spine 29:763–766

19. Pingel A, Kandziora F (2013) Anterior decompression and fusion for cervical neuroforaminal stenosis. Eur Spine J Off Publ Eur Spine Soc Eur Spinal Deform Soc Eur Sect Cerv Spine Res Soc 22:671–672. doi:10.1007/s00586-013-2709-5

20. Hojo Y, Ito M, Abumi K, Kotani Y, Sudo H, Takahata M, Minami A (2011) A late neurological complication following posterior correction surgery of severe cervical kyphosis. Eur Spine J Off Publ Eur Spine Soc Eur Spinal Deform Soc Eur Sect Cerv Spine Res Soc 20:890–898. doi:10.1007/s00586-010-1590-8

21. Nicotra A, Khalil NM, O'Neill K (2011) Cervical radiculopathy: discrepancy or concordance between electromyography and magnetic resonance imaging? Br J Neurosurg 25:789–790. doi:10.3109/02688697.2011.594189

22. Guzman JZ, Baird EO, Fields AC, McAnany SJ, Qureshi SA, Hecht AC, Cho SK (2014) C5 nerve root palsy following decompression of the cervical spine: a systematic evaluation of the literature. Bone Joint J 96-B:950–955. doi:10.1302/0301-620X.96B7.33665

23. Panjabi MM, Maak TG, Ivancic PC, Ito S (2006) Dynamic intervertebral foramen narrowing during simulated rear impact. Spine 31:E128–E134. doi:10.1097/01.brs.0000201243.81745.ba

24. Yoo JU, Zou D, Edwards WT, Bayley J, Yuan HA (1992) Effect of cervical spine motion on the neuroforaminal dimensions of human cervical spine. Spine 17:1131–1136

25. Nuckley DJ, Konodi MA, Raynak GC, Ching RP, Mirza SK (2002) Neural space integrity of the lower cervical spine: effect of normal range of motion. Spine 27:587–595

26. Humphreys SC, Chase J, Patwardhan A, Shuster J, Lomasney L, Hodges SD (1998) Flexion and traction effect on C5–C6 foraminal space. Arch Phys Med Rehabil 79:1105–1109

27. Kitagawa T, Fujiwara A, Kobayashi N, Saiki K, Tamai K, Saotome K (2004) Morphologic changes in the cervical neural foramen due to flexion and extension: in vivo imaging study. Spine 29:2821–2825

28. Muhle C, Resnick D, Ahn JM, Sudmeyer M, Heller M (2001) In vivo changes in the neuroforaminal size at flexion-extension and axial rotation of the cervical spine in healthy persons examined using kinematic magnetic resonance imaging. Spine 26:E287–E293

29. Anderst WJ (2012) Automated measurement of neural foramen cross-sectional area during in vivo functional movement. Comput Methods Biomech Biomed Eng 15:1313–1321. doi:10.1080/10255842.2011.590450